

# Quantum Hall effect at weak magnetic field: New float-up picture

D.N. Sheng<sup>1</sup>, Z.Y. Weng<sup>1</sup>, and X.G. Wen<sup>2</sup>

<sup>1</sup>*Texas Center for Superconductivity, University of Houston, Houston, TX 77204-5506*

<sup>2</sup>*Department of Physics, Massachusetts Institute of Technology, Cambridge, MA 02139*

The fate of integer quantum Hall effect (IQHE) at weak magnetic field is studied numerically in the presence of *correlated* disorders. We find a systematic *float-up* and *merging* picture for extended levels on the low-energy side which results in direct transitions from higher-plateau IQHE states to the insulator. Such direct transitions are controlled by a quantum critical point with a *universal* scaling form of conductance. The phase diagram is in good agreement with recent experiments. The issue of continuum vs. lattice model is also discussed.

73.40.Hm, 71.30.+h, 73.20.Jc

How extended levels evolve with disorders and the magnetic field  $B$  is central to our understanding of the IQHE. Earlier on, Khmel'nitzkii [1] and Laughlin [2] had argued that extended levels should continuously float up towards higher energy with reducing  $B$ . And the assumption that extended levels never merge has led to a select rule of the global phase diagram [3] for IQHE, in which a direct transition from a higher-plateau ( $\nu > 1$ ) state to the insulator is prohibited. But direct transitions have been observed in many recent experiments [4–6], which have renewed the theoretical interest to reexamine the float-up picture in IQHE systems.

Previous numerical studies in the tight-binding model (TBM) with *white-noise* disorders have indicated [7–10] the existence of direct transitions from higher IQHE plateau states to the insulator. But the detailed analysis [8] has also revealed that the lattice effect plays a central role there: such direct transitions first happen near the band center due to the presence of extended levels carrying negative topological Chern number (a peculiar lattice effect) which form a high-energy IQHE-insulator boundary and start to “float-down” towards the low-energy regime with increasing disorder or reducing  $B$ . During the float-down process, the boundary keeps merging with lower extended levels such that the plateaus disappear in a one-by-one fashion.

The key issue is if such a float-down picture, due to the lattice effect, is the unique explanation for direct transitions or there exists a different kind of direct transition free of the lattice effect. Recall that in a continuum model, there does not exist a high IQHE-insulator boundary as the band center is essentially located at infinite energy. In this case a levitation of extended levels by disorders is generally expected as discussed [11,12] perturbatively. Since it has been generally believed that the experimental situation should be physically described by the continuum model due to the weakness of magnetic fields compared to the bandwidth and low density of charge carriers, it becomes especially interesting whether the float-up of extended levels alone can also lead to a direct transition in the low-energy regime.

A float-up of the lowest extended level actually has

been seen in the numerical calculation [10] based on TBM but its journey has quickly ended by merging into the float-down IQHE-insulator boundary from the band center. In order to study how such a float-up feature near the band edge evolves, one has to somehow “delay” the floating-down process of the high IQHE-insulator boundary. Note that the inter-Landau-level-mixing caused by uncorrelated (white-noise) disorders happens more strongly near the band center, which may *enhance* the tendency for extended levels near the band center to move down. So one can try to “smooth” the lattice effect by introducing short-range *correlations* among disorders. As a result to be shown below, a float-up process will then become a dominant effect for those *lower* extended levels as the float-down of the high IQHE-insulator boundary is significantly slowed, in contrast to the case in the white-noise limit [7–9] at similar weak magnetic fields.

In this Letter, we present a systematic floating-up and *merging* pattern revealed for extended levels near the band edge. Specifically, the lowest extended level starts to float upward at stronger disorder or weaker  $B$  and eventually emerges into the second lowest extended level to form a *new* IQHE-insulator boundary on the low-energy side, leading to a  $\nu = 2 \rightarrow 0$  direct transition, while the aforementioned *upper* IQHE-insulator boundary still remains at high energy. And such a lower IQHE-insulator boundary keeps moving up to merge with higher-energy extended levels to result in  $3 - 0$ ,  $4 - 0$ , ... direct transitions with increasing disorders or reducing  $B$ . The phase diagram is in good agreement with the experiments. Furthermore, direct transitions to the insulator at the lower boundary are found to be consistent with a quantum critical point picture, and in particular the conductance as a function of  $B - B_c$  ( $B_c$  denotes the critical magnetic field) is of the *universal* form for  $1 - 0$ ,  $2 - 0$ , ... up to  $6 - 0$  transitions within the numerical resolutions.

The TBM model  $H = -\sum_{\langle ij \rangle} e^{ia_{ij}} c_i^+ c_j + H.c. + \sum_i w_i c_i^+ c_i$ , with the magnetic flux per plaquette  $\phi = \sum_{\square} a_{ij} = 2\pi m/M$  ( $m$  and  $M$  are integers). And we define  $B = m/M$ . The correlated disorder  $w_i$  is generated

by  $w_i = W/\pi \sum_j f_j e^{-|\mathbf{R}_i - \mathbf{R}_j|^2/\lambda_0^2}$ . Here  $\mathbf{R}_i$  denotes the spatial position of site  $i$ .  $W$  and  $\lambda_0$  are the strength and correlation length scale of disorders, respectively.  $f_i$  is a random number distributing uniformly between (-1,1).

To illustrate how extended levels near the band edge evolve with the disorder strength  $W$ , the density of states carrying nonzero Chern number ( $\rho_{ext}$ ) as a function of the Landau level filling number ( $n_L$ ) is plotted in Fig. 1 (a) and (b) at  $B = 1/64$ ,  $\lambda_0 = 1$ , and the sample size  $32 \times 64$ . The sample-size-independent peaks in the figures denote the positions of extended levels while the non-peak part of  $\rho_{ext}$  should scale to zero presumably in the thermodynamic limit [8,13]. In Fig. 1(a), as  $W$  is increased from 0.7 to 1.4, extended level positions (marked by diamonds) all start to *float up* slightly from the filling number  $n_L = \nu + 0.5$  ( $\nu = 0, 1, \dots$ ). But the lowest extended level distinctly moves faster and eventually *merges* into the second lowest extended level to form a new boundary extended level [see  $W = 1.45$  and 1.55 cases in Fig. 1(b)], while the higher extended levels still remain roughly equally spaced (note that in this strong disorder case, the merged peak of  $\rho_{ext}$  becomes less significant but later we will discuss a more reliable way to identify the extended levels). It corresponds to the *collapse* of the mobility gap separating the lowest two neighboring extended levels and thus the *destruction* of the  $\nu = 1$  IQHE plateau in between. By further increasing  $W$ , we see that such a newly merged extended level boundary continuously floats up and merges into the third extended level, and so on and so forth. In this way, the IQHE plateaus disappear on the low  $n_L$  side also in a one by one fashion. We emphasize that higher extended levels originally at  $n_L = \nu + 0.5$  ( $\nu \geq 1$ ) never move passing the  $n_L = \nu + 1$  before merging with the lower boundary [Fig. 1(b)] such that each IQHE plateau does not really float away before its destruction.

Such a float-up and merging picture persists into very weak magnetic fields (from  $B = 1/64$  to  $B = 1/2304$ ). The disorder strength  $W_c$  at which the merged lowest two extended levels pass  $n_L = 2$ , resulting in a  $2 - 0$  transition, is shown in the inset of Fig. 1(c) as a function of  $B$ . We see that  $W_c$  monotonically decreases with  $B$  and is extrapolated to zero in zero  $B$  limit in a fashion of  $B^{1/2}$ .

By following the trace of extended levels in the  $n - B$  plane ( $n$  is the on-site electron density) at fixed  $W = 1.4$  and  $\lambda_0 = 1$ , we determine a phase diagram in Fig. 1(c), where the filled circles represent the lower IQHE-insulator boundary, while the open circles are the positions of various extended levels between plateaus which merge into the boundary at weaker  $B$ . This phase diagram is very similar to the recent experimental phase diagram [Fig. 2 in Ref. [4]] as well as the earlier one obtained in Ref. [5,6]. The Hall conductance calculation confirms that  $\sigma_{xy}$  indeed saturates to  $\nu e^2/h$  in  $\nu$ -th plateau region while it approaches zero on insulating side. Both critical

conductances  $\sigma_{xxc}$  and  $\sigma_{xyc}$  at  $\nu \rightarrow 0$  transition are close to  $\nu e^2/2h$  in accordance with experiments [6].

Apparently the above results critically depend on how reliably one can identify the positions of extended levels using finite-size calculations. Let us focus on the merged extended levels as the lower IQHE-insulator boundary shown in Fig. 1(c). By fixing  $n_L = 2$ , marked by the arrow  $C$  in Fig. 1(c), we calculated the longitudinal conductance  $\sigma_{xx}$  with  $B$  changing continuously at fixed  $W = 1.4$ . We found a peak in  $\sigma_{xx}$  at  $B_c = 1/70$  as a  $2 - 0$  transition. In Fig. 2(a),  $\sigma_{xx}$  as a function of  $B$  with  $n_L = 1, 2, \dots$ , and 6 at  $W = 1.4$  are shown for sample width  $L = 96$  (the stripe sample with  $L_x = L$  and  $L_y \sim 10^6$  is considered using transfer matrix method [14]). The  $L$ -independent peak positions should correspond to  $\nu = 1 \rightarrow 0, 2 \rightarrow 0, \dots$ , and  $6 \rightarrow 0$  transitions in Fig. 1(c). Remarkably, all these data can be collapsed onto a universal curve

$$\sigma_{xx}/\sigma_c = 2 \exp(s)/(1 + \exp(2s)), \quad (1)$$

as shown in Fig. 2(b) if one defines a variable  $s = c_\nu(L)(B - B_c)/B_c$ . Here the parameter  $1/c_\nu(L)$  represents the relative width of  $\nu \rightarrow 0$  transition at a finite  $L$ . Furthermore, by collapsing the data at different  $L$ 's, we find a scaling curve for  $\nu = 2 \rightarrow 0$  transition in Fig. 3(a), with

$$c(L) \propto L^{1/x} \quad (2)$$

from  $L = 32$  to  $L = 160$ . The correlation length exponent is identified to be  $x = 4.6 \pm 0.5$  in the inset of Fig. 3(a), about doubled from  $x = 2.3$  for the  $\nu = 1 \rightarrow 0$  transition which has been similarly determined at  $n_L = 1$ . The exponents for  $3 - 0, \dots, 6 - 0$  transitions seem further increased but are more difficult to determine with a similar accuracy for larger sample sizes are needed. It is noted that the scaling form (1) is not limited to  $n_L = \text{integer}$ . For example, the data at  $\nu = 2 \rightarrow 0$  transition with  $n_L = 2.2$  can be also collapsed onto the same curve. Furthermore, Eq.(1) still holds as we change  $\lambda_0$  from 1 to 2 and 3. Details will be presented elsewhere.

Based on (1) and (2), we conclude that the  $\nu = 2 \rightarrow 0$  transition corresponds to a quantum critical point with measure zero in the  $L \rightarrow \infty$  limit. We note that the same scaling form has been previously obtained [15] for the  $1 - 0$  transition, where  $\rho_{xx} = \exp(-s) \frac{h}{e^2}$  and  $\rho_{xy} = \frac{h}{e^2}$  leading to (1). Identifying such a simple scaling relation for  $\nu = 1, 2 \rightarrow 0$  as well as higher plateaus to insulator transitions may be the most striking evidence for a single quantum critical point at each transition. The standard scaling method can be also applied to the  $\nu = 2 \rightarrow 0$  transition to *independently* verify the one parameter scaling law [16]. As shown in Fig. 3(b), by collapsing the same data as  $\sigma_{xx}(L)/\sigma_c = f(\xi/L)$  by a correlation length  $\xi$ , we find  $\xi \propto |(B - B_c)/B_c|^{-x}$  with  $x = 4.5 \pm 0.5$  [the inset of Fig. 3(b)] in agreement with the above result.

We have also checked the case right before the lowest two extended levels merge together. By scanning  $B$  at a fixed  $n_L = 1.8$  nearby the scan  $C$  shown in Fig. 1(c),  $\sigma_{xx}$  exhibits two distinct peaks at  $B_{c1} = 0.0151$  and  $B_{c2} = 0.0169$  with  $L = 128$  [see the middle inset of Fig. 4(a)]. The main panel of Fig. 4(a) shows the finite-size scaling curve of  $\sigma_{xx}/\sigma_c$  as a function of  $\xi/L$  obtained by collapsing the data of different sample sizes at  $B < B_{c1}$ . The right inset indicates that  $\xi$  diverges at  $B_{c1}$  with an exponent  $x = 2.4$  which is essentially the same as the standard one for the 1–0 transition. Similar finite-size scaling curve has been also obtained for the branch at  $B > B_{c2}$ , corresponding to the 2–1 transition. It is noted that the above analysis resembles the study [17] of the spin unresolved case at strong magnetic field where a small spin-orbit coupling is used to lift the spin degeneracy to create two separated but very close quantum critical points. Similar to the latter case, if one “mistakenly” treats the present case as a *single* critical point at  $B_m$ , a middle point between  $B_{c1}$  and  $B_{c2}$ , and proceeds with a finite-size scaling analysis, then one gets Fig. 4(b) where the quality of data collapsing becomes markedly worse and in particular  $\xi$  shows a saturation trend approaching  $B_m$ , contrary to the assumption of a critical point at  $B_m$ . Thus, the two separated extended levels with  $|B_{c1} - B_{c2}|/B_m \sim 0.11$  is not mistakable as a single critical point in our numerical analysis. Finally, we make a remark that even if the 2–0 transition that we observed is actually two transitions with very small  $|B_{c1} - B_{c2}|$  indistinguishable numerically, the nice scaling properties [(1) and (2)] that we found still indicate that there is a new quantum critical point. In this case, the splitting  $|B_{c1} - B_{c2}| \neq 0$ , if it exists, should be caused by a relevant operator of such a new critical point.

To summarize, we have identified for the first time a new float-up and merging pattern for extended levels near the band edge at weak  $B$  (down to  $B = 1/2304$  where there are 1252 Landau levels between the band edge and center). The corresponding phase diagram with direct transitions is in excellent agreement with the experiments where the essential features can be explained by the narrowing and destruction of each IQHE plateau due to the sequential merging of neighboring extended levels as the mobility gap in between collapses.

**Acknowledgments** - D.N.S. would like to acknowledge helpful discussions with R. N. Bhatt, F.D.M. Haldane, and M. Hilke. D.N.S. and Z.Y.W. are supported by the State of Texas through ARP Grant No. 3652707 and TCSUH. X.G.W. is supported by NSF Grant No. DMR-97-14198 and NSF-MRSEC Grant No. DMR-98-08941.

- [1] D. E. Khmel'nitzkii, Phys. Lett. **106A**, 182 (1984).
- [2] R. B. Laughlin, Phys. Rev. Lett. **52**, 2304 (1984).
- [3] S. A. Kivelson, D. -H. Lee, and S. -C. Zhang, Phys. Rev. B, **46**, 2223 (1992);
- [4] M. Hilke et al., preprint cond-mat/9906212.
- [5] S. V. Kravchenko et al., Phys. Rev. Lett. **75**, 910 (1995); A. A. Shashkin, G. V. Kravchenko, and V. T. Dolgopolov, JETP Lett. **58**, 220 (1993); V. M. Pudalov et al., Sur. Sci. **305**, 107 (1994).
- [6] S. -H. Song et al., Phys. Rev. Lett. **78**, 2200 (1997); D. Shahar et al., Phys. Rev. B **52**, R14372 (1995).
- [7] D. Z. Liu, et al., Phys. Rev. Lett. **76**, 975 (1996).
- [8] D. N. Sheng and Z. Y. Weng, Phys. Rev. Lett. **78**, 318 (1997).
- [9] H. Potempa et al., Physica B **256**, 591 (1998); Y. Hatsugai, K. Ishibashi, and Y. Morita, to appear in Phys. Rev. Lett. (1999).
- [10] D. N. Sheng and Z. Y. Weng, preprint cond-mat/9906261.
- [11] F. D. M. Haldane and K. Yang, Phys. Rev. Lett. **78**, 298 (1997).
- [12] M. M. Fogler, Phys. Rev. B **57**, 11947 (1998).
- [13] K. Yang and R. N. Bhatt, Phys. Rev. Lett. **76**, 1316 (1996); Phys. Rev. B **59**, 8144 (1999).
- [14] A. MacKinnon and B. Kramer, Z. Phys. **53**, 1 (1983).
- [15] D. N. Sheng and Z. Y. Weng, Phys. Rev. Lett. **83**, 144 (1999); D. N. Sheng and Z. Y. Weng, Phys. Rev. B **59**, R7821 (1999).
- [16] B. Huckestein and B. Kramer, Phys. Rev. Lett. **64**, 1437 (1990).
- [17] Z. Wang, D. -H. Lee, and X. -G. Wen, Phys. Rev. Lett. **72**, 2454 (1994).

Fig. 1. (a) The postions of extended levels determined by the peaks (filled  $\diamond$ ) of the density of states with nonzero Chern number (see text). (b) Float-up and merging pattern of extended levels with the increase of the disorder strength  $W$ . (c) The numerical phase diagram in electron density - magnetic field ( $n$ - $B$ ) plane at  $\lambda_0 = 1$ . The inset: The critical disorder  $W_c$  for  $\nu = 2 \rightarrow 0$  transition at  $n_L = 2$  as a function of  $B$ .

Fig. 2. (a) The single-peak behavior of the longitudinal conductance  $\sigma_{xx}$  versus  $B$ , corresponding to the lowest six plateaus to the insulator transitions at fixed  $n_L = 1, 2, \dots, 6$ , respectively. (b) The normalized conductance  $\sigma_{xx}/\sigma_c$  ( $\sigma_c$  is the peak value) versus a scaling variable  $s = c_\nu(L)(B - B_c)/B_c$  which follows a universal function form (1).

Fig. 3. (a) The normalized conductance  $\sigma_{xx}(L)/\sigma_c$  for  $\nu = 2 \rightarrow 0$  transition at different sample sizes. The inset:  $c(L) = c_0 L^{1/x}$  where  $x = 4.6 \pm 0.5$ . (b) The same data are collapsed as a function of  $\xi/L$ . The inset:  $\xi \propto |B - B_c|^{-x}$ .

Fig. 4. The double-peak  $\sigma_{xx}$  before two lowest extended levels merge is shown in the middle panel of (a). (a)  $\sigma_{xx}/\sigma_c$  as a function of  $\xi/L$  by collapsing all the data at  $B < B_{c1}$  with  $\xi$  shown in the right inset. (b) By assuming a single critical point at  $B_m$ , the data collapsing shows worse quality and  $\xi$  in the inset becomes saturated approaching  $B_m$ .

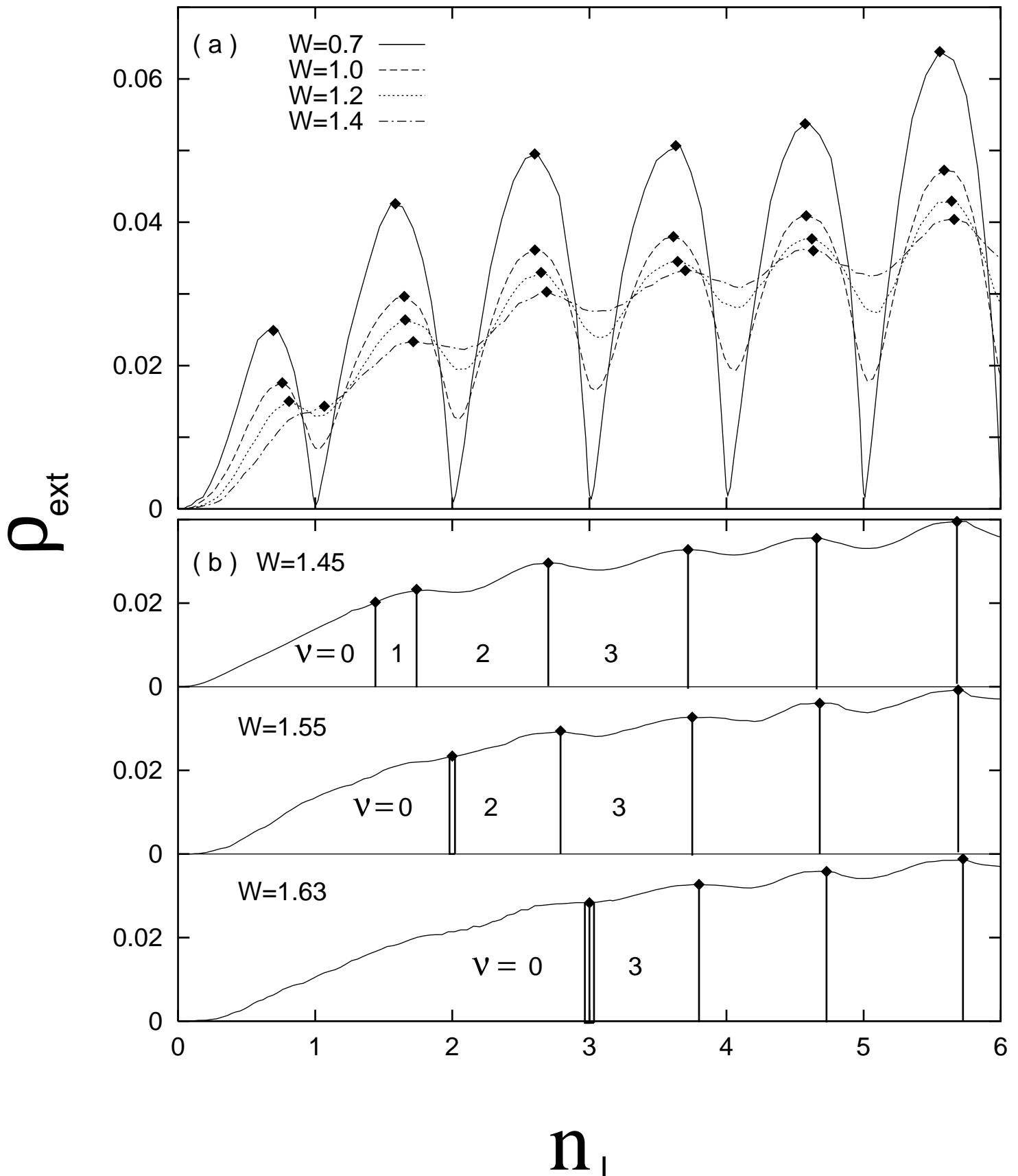


Fig. 1(a), (b)

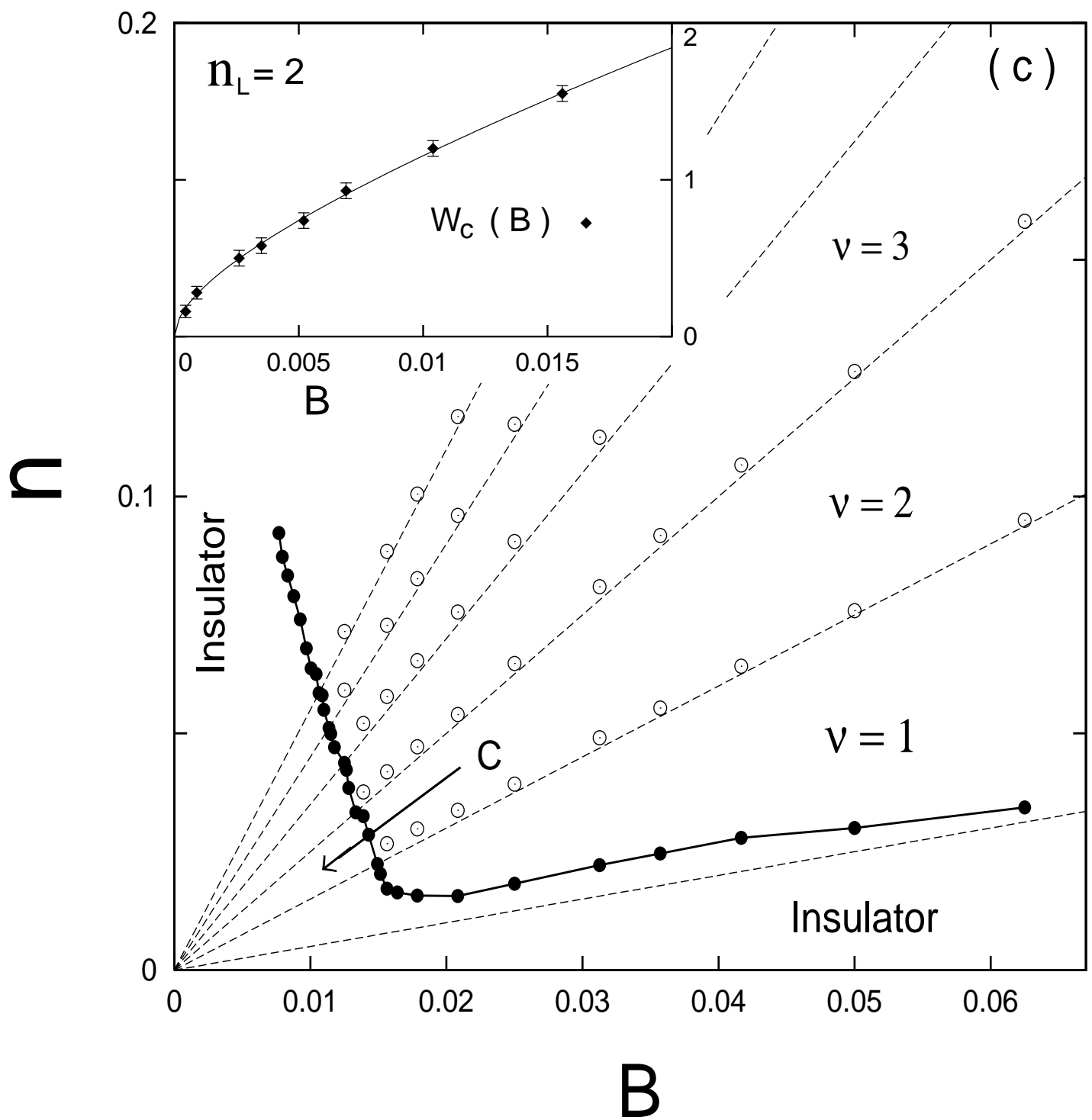


Fig. 1c

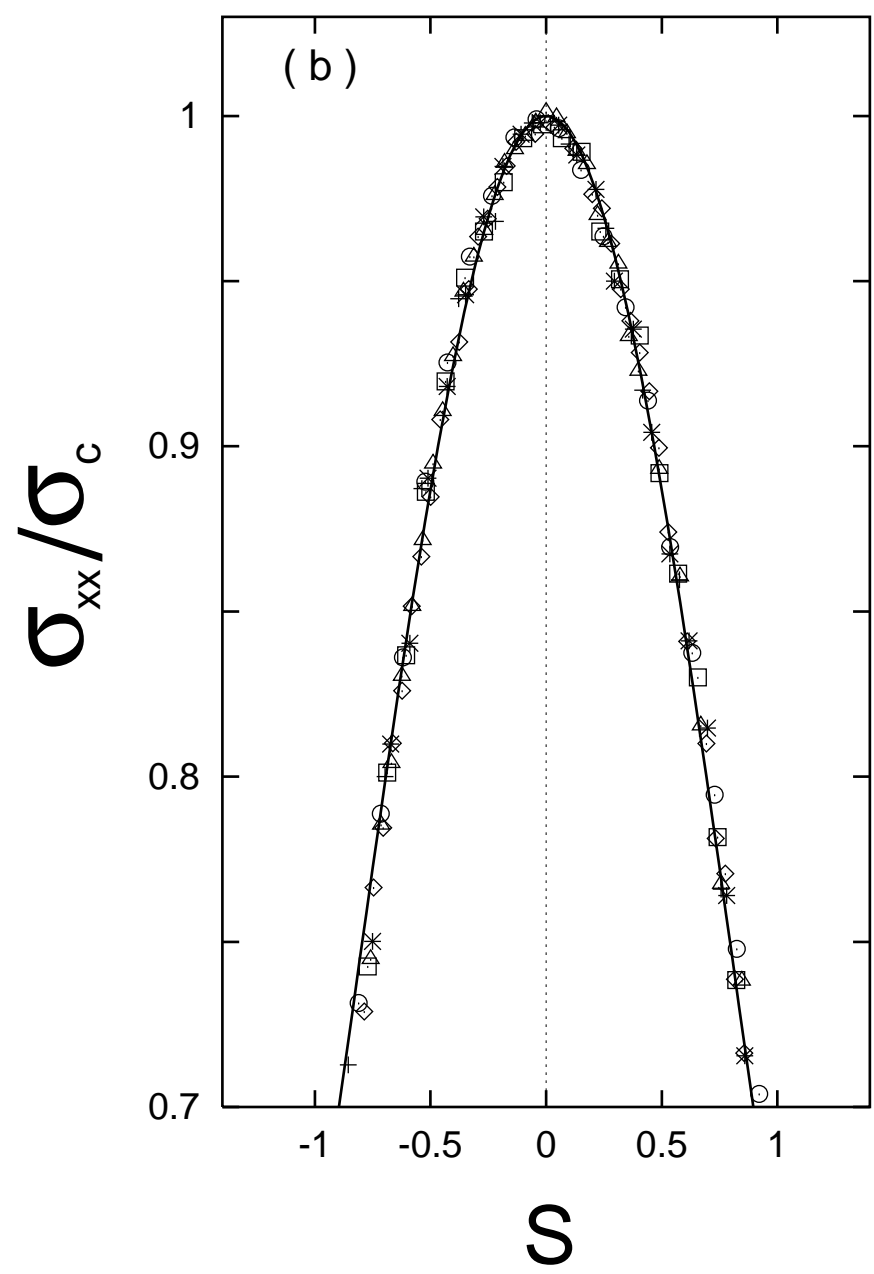
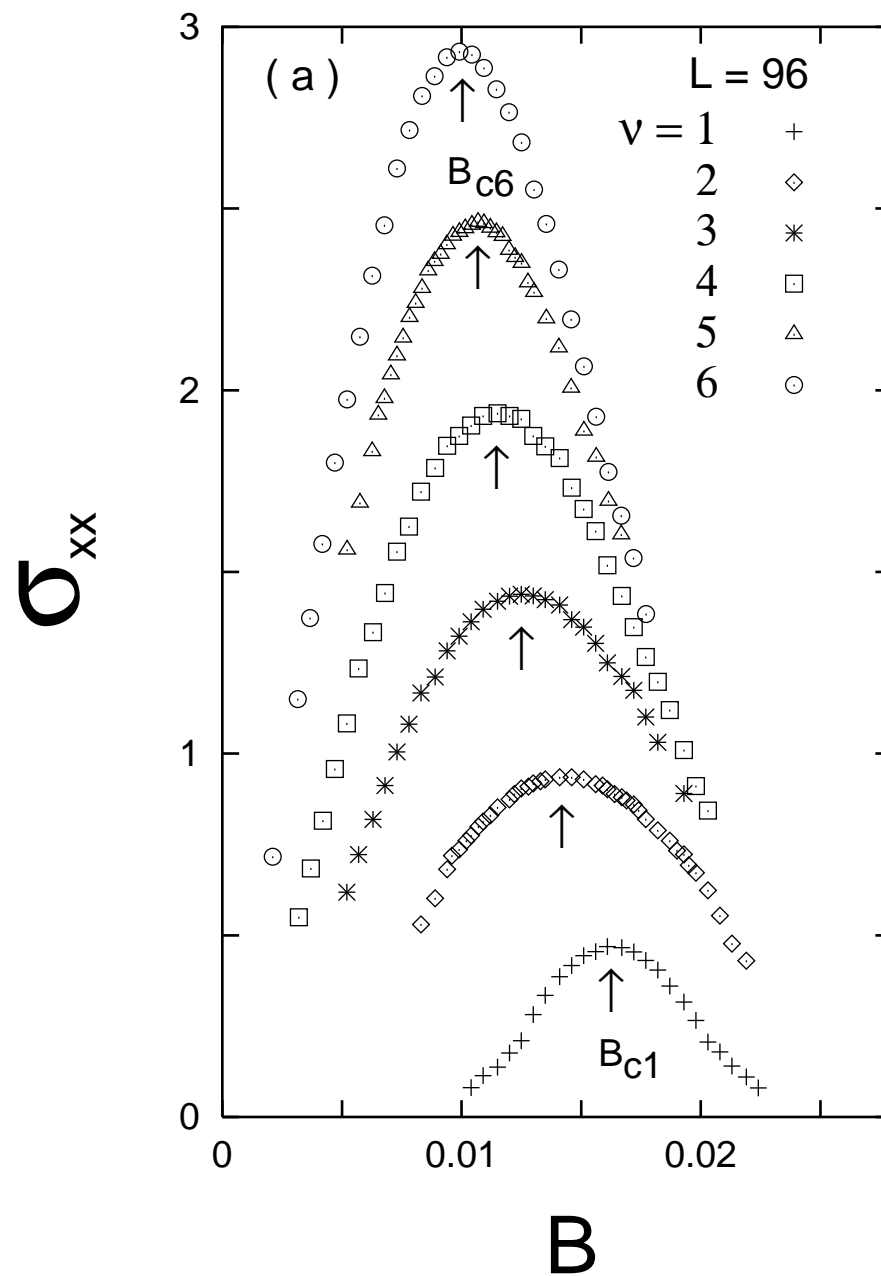


Fig. 2

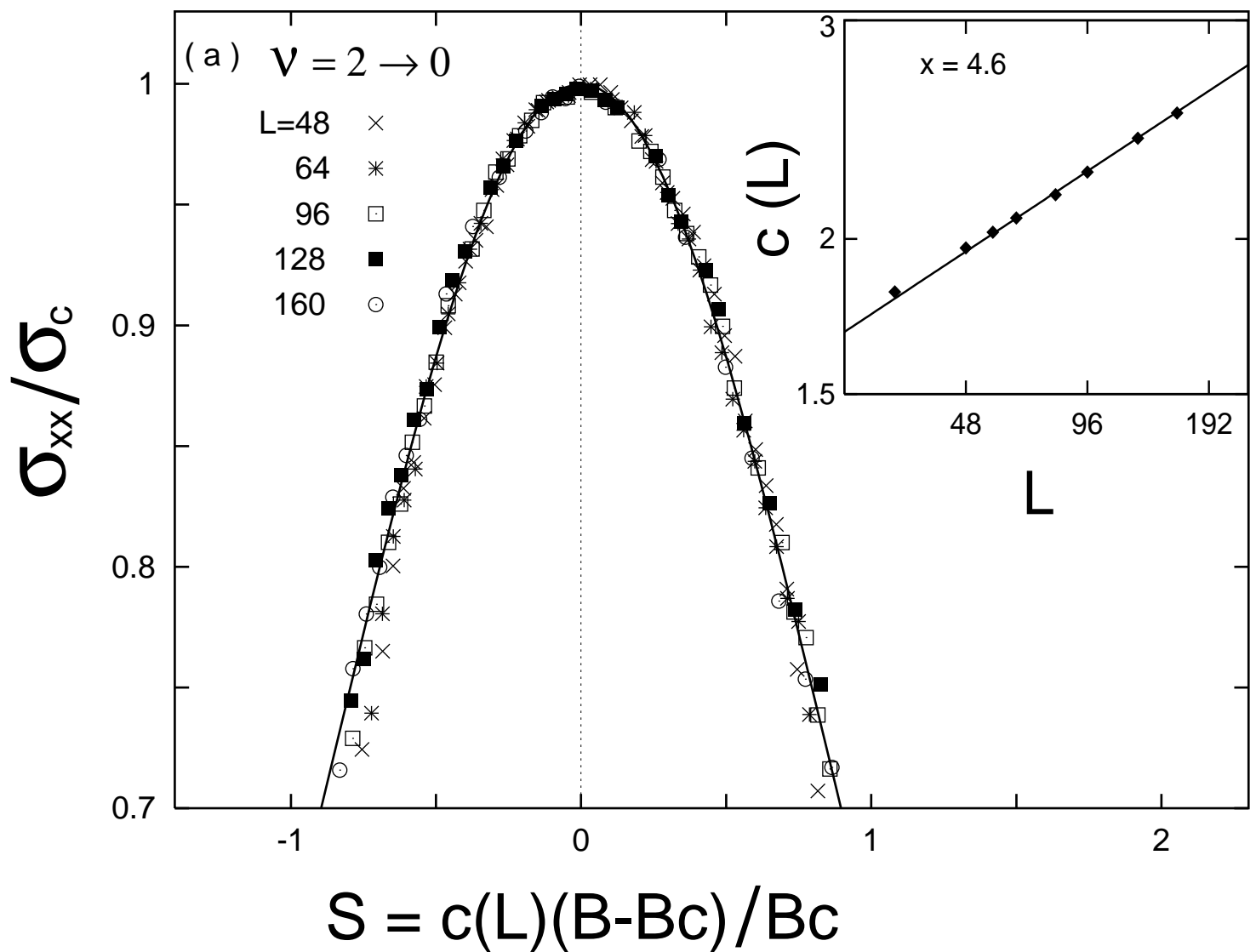


Fig. 3 (a)

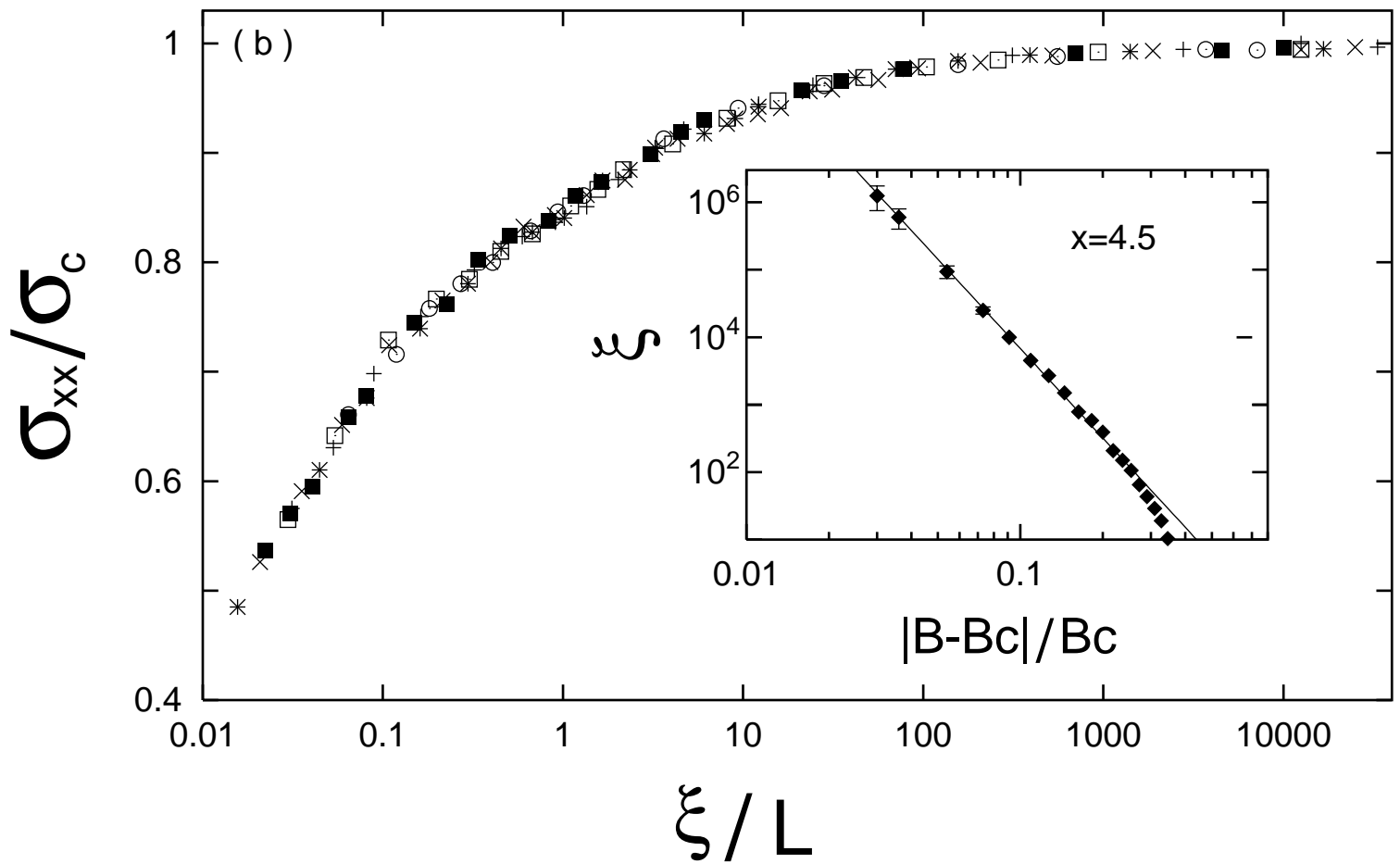
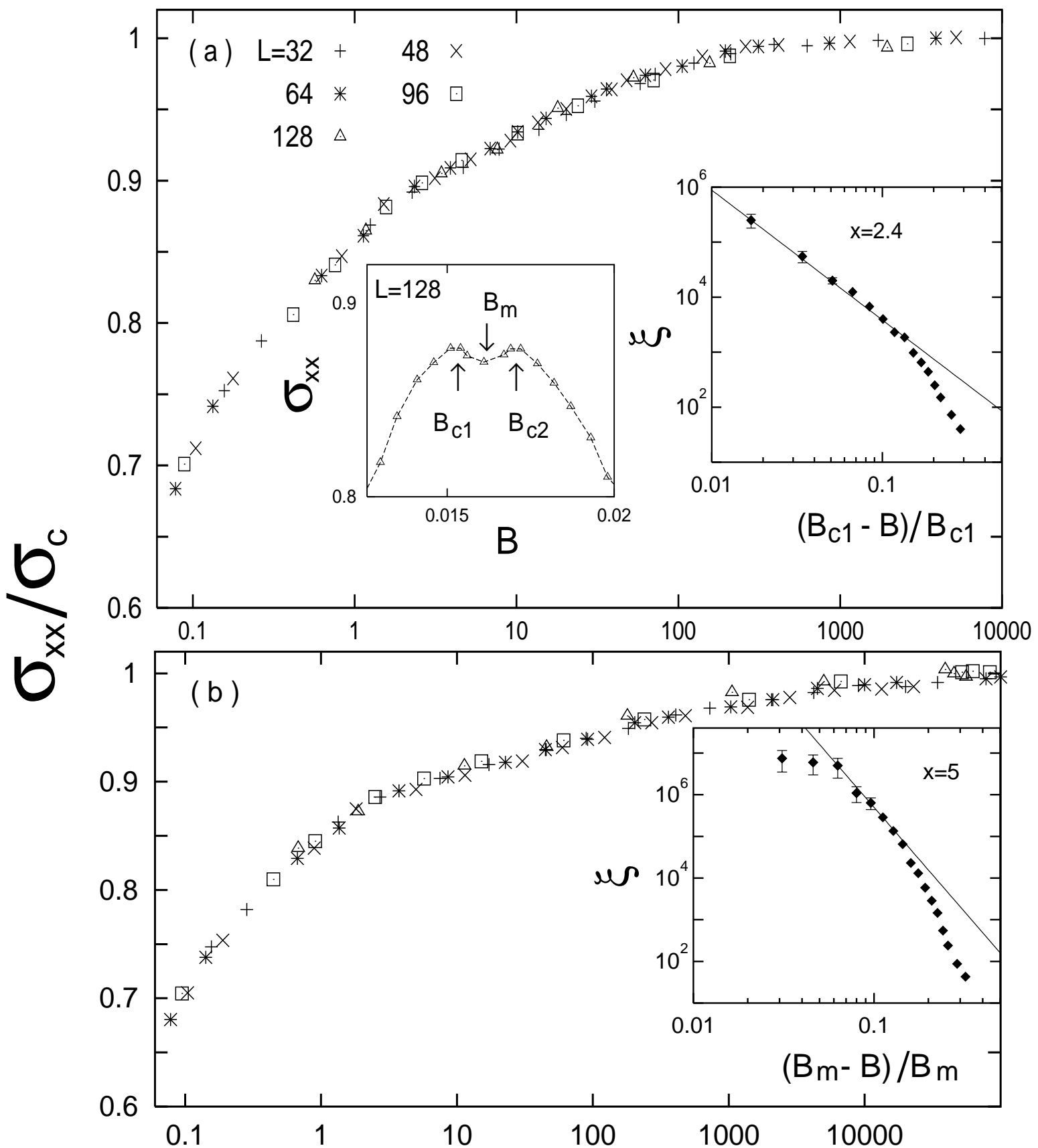


Fig. 3 (b)



$\xi / L$

Fig. 4